

How far can we see back in time in high-energy collisions using charm quarks?

László Gyulai^{1,2,*} Gábor Bíró^{2,3,†} Róbert

Vértesi^{2,‡} and Gergely Gábor Barnaföldi^{2,§}

¹*Budapest University of Technology and Economics,
Műegyetem rkp. 3., H-1111 Budapest, Hungary.*

²*HUN-REN Wigner Research Center for Physics,
29–33 Konkoly-Thege Miklós Str., H-1121 Budapest, Hungary.*

³*ELTE Eötvös Loránd University, Institute of Physics,
1/A Pázmány Péter Sétány, H-1117 Budapest, Hungary.*

(Dated: January 26, 2024)

Abstract

We use open charm production to estimate how far we can see back in time in high-energy hadron-hadron collisions. We analyze the transverse momentum distributions of the identified D mesons from pp, p-Pb and A-A collisions at the ALICE and STAR experiments covering the energy range from $\sqrt{s_{\text{NN}}} = 200$ GeV up to 7 TeV. Within a non-extensive statistical framework, the common Tsallis parameters for D mesons represent higher temperature and more degrees of freedom than that of light-flavour hadrons. The production of D mesons corresponds to a significantly earlier proper time, $\tau_{\text{D}} = (0.18 \pm 0.06)\tau_{\text{LF}}$.

INTRODUCTION

In the theory of strong interaction, quantum chromodynamics (QCD), quarks and gluons at low energy exist in colour singlet states, confined into hadrons. However, in the extreme conditions of high-energy heavy-ion collisions, quark-gluon plasma (QGP) can be formed, which is a state of matter where these partons exist in a deconfined phase with colour degrees of freedom. This unique plasma state is believed to have existed microseconds after the Big Bang, offering a glimpse into the primordial Universe. In recent decades, experiments conducted at the Relativistic Heavy Ion Collider (RHIC) and the Large Hadron Collider (LHC) have played a pivotal role in advancing our understanding of the QGP by systematically measuring many of its fundamental properties [1–6]. These experiments observed a strong collectivity in high-energy heavy-ion collisions, which has been attributed to a strongly coupled QGP. More recently, collective phenomena have also been observed in smaller collision systems, such as proton-nucleus (p-A) or even proton-proton (pp) [7–9]. Similarly, an enhancement of strangeness production has also been seen in pp systems [10]. Whether QGP droplets can come into existence in small systems, or the observed collectivity is a result of complex vacuum-QCD effects is still an open question, and description of the observations in a unified framework poses a challenge for theories [11–13].

In a high-energy collision, light-flavour and strange hadrons¹ mostly carry information

* gyulai.laszlo@wigner.hun-ren.hu

† biro.gabor@wigner.hun-ren.hu

‡ vertesi.robert@wigner.hun-ren.hu

§ barnafoldi.gergely@wigner.hun-ren.hu

¹ From here on we refer to them simply as light-flavour hadrons.

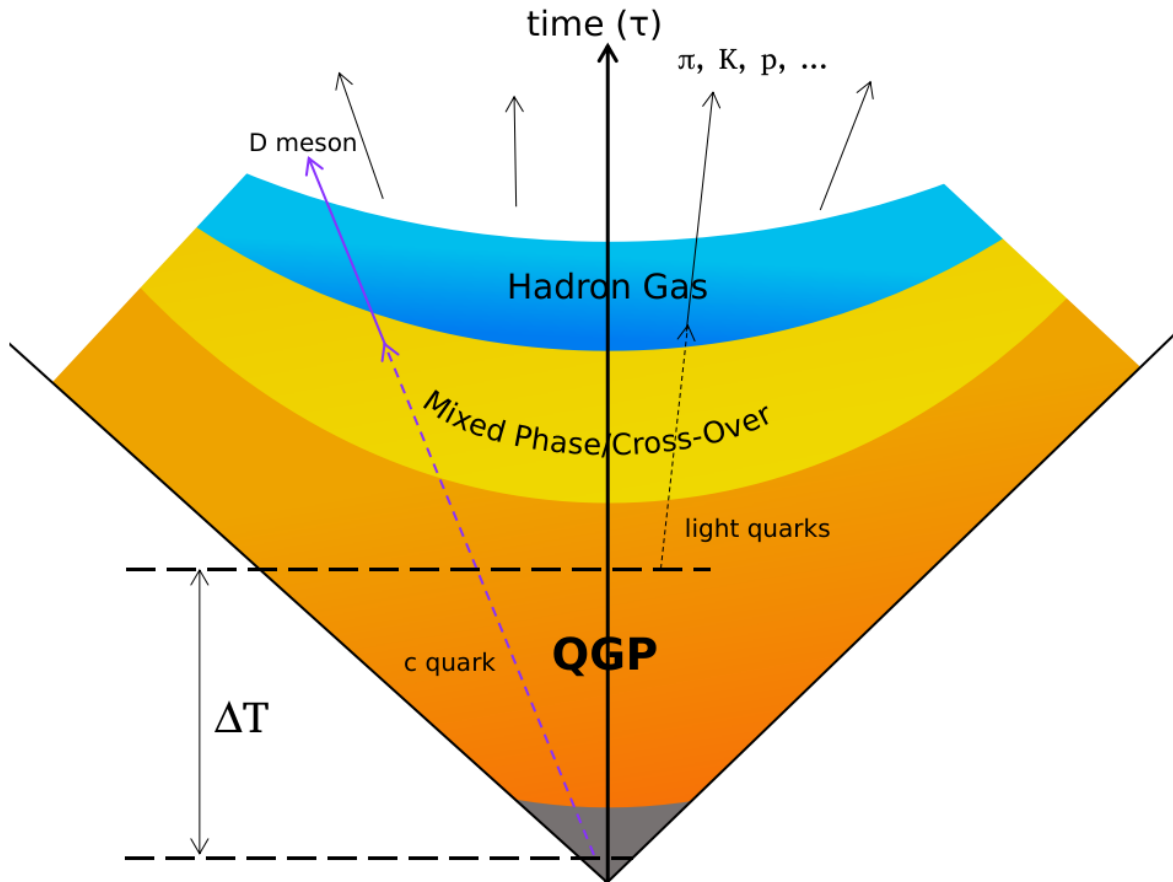


FIG. 1. Schematic view of the evolution of matter in a high-energy nucleus-nucleus collision. Heavy c quarks are produced in the initial stages, while light quarks are formed in the QGP phase. Later, during the phase transition, quarks combine to form hadrons.

about the final state [14]. By detecting heavy-flavour hadrons, however, one can learn about the earlier stages of the reaction as well. The heavy-flavour charm (c) and beauty (b) quarks are produced in the initial stages of the collisions. Since they have a very long lifetime and negligible annihilation cross section, they survive the collision and experience the whole evolution of the system [15–17]. In pp collisions they serve as a testbench for QCD, since the processes can be perturbatively described down to low momenta. In heavy-ion collisions, however, they come into contact with the QGP through collisional and radiative interactions before thermalizing and forming hadrons, therefore they bring information about the whole evolution of the QGP (Fig. 1). Recent development of detector capabilities allows for high-precision measurements of heavy-flavour hadrons over a broad range of transverse mo-

mentum (p_T) down to fractions of GeV. The most common heavy-flavour hadrons, emerging from open charm processes, are the D^0 , D^+ and D^{*+} mesons consisting of a c quark and a light antiquark, and their antiparticles (collectively referred to as D mesons). The identified spectra of D mesons were measured at RHIC and LHC energies in several collisional systems with high precision, which allows for a thorough comparison of light and heavy-flavour hadron production at the next upgrade phase of the ALICE detector [18] or the proposed ALICE 3 [19].

Spectra of identified particles produced in high-energy collisions comprise soft thermally produced particles, as well as particles from hard QCD processes. The non-extensive Tsallis – Pareto statistical framework describes these two components of the spectra in a unified way, independently of their formation process [20–22]. The Tsallis-thermometer proved to be a sensitive tool to learn about the system size and/or fluctuations and correlations in the system. This was proposed by Bíró *et al.* [23]. However, the method had been previously applied only to light-flavour hadrons, therefore the results are mostly representative of the final state. In the current work, we use D mesons to investigate the thermodynamical properties of earlier stages of the system.

METHOD

The transverse momentum distributions of charged and identified hadrons, yielding from energetic collisions of hadrons or heavy nuclei, provide details about particle creation processes and the properties of QCD matter that may be produced in such reactions. The soft, low- p_T part of the spectrum is associated with the particles stemming from a thermal equilibrium. This part is well described by Boltzmann – Gibbs statistics, characterized by the kinetic freeze-out temperature parametrizing the exponential function [24, 25]. On the other hand, the jetty, high- p_T regime of the spectrum follows a power-law-like distribution, inherited from perturbative QCD hadron production [26].

The Tsallis – Pareto family of distributions, derived from the generalization of the traditional Boltzmann – Gibbs entropy, successfully unite the two regions of the spectrum [20–22]. It has been shown in several recent studies that various parametrizations of these distributions fit well to the measured data from RHIC to LHC energies [20, 23, 26–33]. In the present work, we consider a thermodynamically-motivated and consistent form of the distribution

to fit the invariant yield of identified hadrons at mid-rapidity:

$$\left. \frac{d^2N}{2\pi p_T dp_T dy} \right|_{y \approx 0} \equiv \quad (1)$$

$$Am_T f^q = Am_T \left[1 + \frac{q-1}{T} (m_T - \mu) \right]^{-\frac{q}{q-1}},$$

where $A = gV/(2\pi)^3$ is the normalization factor containing the volume V and degeneracy factor g ; q and T are the non-extensivity parameter and the Tsallis temperature, respectively; $m_T = \sqrt{p_T^2 + m^2}$ is the transverse mass, and the chemical potential μ is approximated as the rest mass of the given hadron, $\mu \approx m$. Following the works of [23, 34–36], we can define the Tsallis parameters from the event-by-event fluctuations of the number of the produced particles, n :

$$T = \frac{E}{\langle n \rangle}, \quad (2)$$

$$q = 1 - \frac{1}{\langle n \rangle} + \frac{\Delta n^2}{\langle n \rangle^2}. \quad (3)$$

This leads to an energy-dependent linear correlation between the Tsallis parameters

$$T = E(\delta^2 - (q - 1)), \quad (4)$$

where the relative size of multiplicity fluctuations $\delta^2 := \frac{\Delta n^2}{\langle n \rangle^2}$ is assumed to be constant.

In Ref. [23] we have shown that the Tsallis parameters indeed present strong correlations with the average event multiplicity, spanning through several collision systems. For identified light-flavour hadrons the Tsallis parameters also exhibit a scaling behaviour in charged-hadron multiplicity ($N_{\text{ch}} \sim n$), as well as in collision energy ($\sqrt{s_{\text{NN}}}$). The scaling results in a grouping of the Tsallis parameters T and q towards low event multiplicities, around the values $T_{\text{eq}} = 0.144 \pm 0.010$ GeV and $q_{\text{eq}} = 1.156 \pm 0.007$. However, as the production time-scale (and consequently, the carried information about interacting material) of heavy-flavour hadrons is different, it is an interesting opportunity to quantitatively examine these hadron species with respect to the Tsallis-thermometer.

RESULTS AND DISCUSSION

In the current study, we analyzed 11 datasets of pp, p–Pb, Au–Au and Pb–Pb collision systems at various center-of-mass energies from the publicly available measurements of ALICE and STAR experiments. From the pp collisions at $\sqrt{s} = 5.02$ TeV and 7 TeV energies

from the ALICE experiment we investigated the minimum-bias spectra of D^0 , D^+ , and D^{*+} mesons [37, 38]. The spectra of the same three meson species were also taken from the p–Pb collisions at $\sqrt{s_{NN}} = 5.02$ TeV energy from ALICE [39]. We also studied two centrality-dependent (and consequently multiplicity-dependent) D^0 -meson datasets of A–A systems. One of them was the Au–Au system at $\sqrt{s_{NN}} = 200$ GeV energy from the STAR with a total of 5 centrality classes: 0–10%, 10–20%, 20–40%, 40–60%, 60–80% [40]. The other one was Pb–Pb at $\sqrt{s_{NN}} = 2.76$ TeV center-of-mass energy from the ALICE experiment with 0–20% and 40–80% centrality classes [41]. All the spectra cover a broad range of transverse momentum over a large number of data points, which allows for a precise application of the Tsallis–Pareto fit [28].

The investigated D-meson datasets were fitted with the Tsallis–Pareto distribution using the LMFIT: Non-Linear Least-Squares Minimization and Curve-Fitting for Python package [42]. At first, the low- and high- p_T regions were fitted separately, after which the results of these fits were used as an input for the fit of the whole spectrum. This method proved to be stable and provided good χ^2/ndf values. The fit parameters are summarized in Table I, while the fitted spectra are shown in Appendix A.

Following the method developed in Ref. [23], we evaluated the consistency of the thermodynamical variables by verifying that the first law of thermodynamics with a first order Euler equation

$$\epsilon + P - Ts - \mu n = 0 \quad (5)$$

is fulfilled. We found that the consistency is fulfilled for light-flavour mesons within 1% precision. For heavier hadrons this can deviate slightly more, however, for D mesons it always stays below 8%. The details of this procedure are presented in Appendix B.

The T and q parameters, extracted from the D-meson fits, are presented in the Tsallis-thermometer, $T - (q - 1)$ diagram shown in Fig. 2 alongside the parameters from the light-flavour study [23], which are drawn without error bars and with semi-transparent colours for better visibility.

For the case of light-flavour hadrons, a mass hierarchy had been observed: the parameter T shows an increasing trend both with particle mass and with event multiplicity within the same particle species, while the parameter q is decreasing in the same manner. This behaviour becomes more distinct for heavy hadrons, and is similarly observed for the D mesons. Strong dependence on multiplicity for heavy-flavour hadrons is also present.

TABLE I. Parameters of Tsallis fits on D-meson spectra.

$\sqrt{s_{\text{NN}}}$ (GeV)	Hadron	$\left\langle \frac{dN_{\text{ch}}}{d\eta} \right\rangle$	T (GeV)	q	χ^2/ndf
AuAu, 200	D^0	680.0	0.32 ± 0.01	1.06 ± 0.01	4.1/8
		424.5	0.36 ± 0.03	1.05 ± 0.02	15.6/8
		235.7	0.31 ± 0.01	1.07 ± 0.01	12.7/8
		90.0	0.32 ± 0.02	1.09 ± 0.01	13.8/8
		27.0	0.29 ± 0.04	1.12 ± 0.03	29.2/8
PbPb, 2760	D^0	600.0	0.32 ± 0.06	1.16 ± 0.02	0.9/4
		45.0	0.23 ± 0.05	1.21 ± 0.02	0.9/4
pp, 5020	D^0		0.45 ± 0.01	1.16 ± 0.01	7.8/18
	D^+		0.43 ± 0.02	1.16 ± 0.01	15.9/17
	D^{*+}		0.44 ± 0.02	1.17 ± 0.01	11.6/16
pPb, 5020	D^0		0.43 ± 0.02	1.17 ± 0.01	199.7/18
	D^+		0.38 ± 0.03	1.17 ± 0.01	792.3/17
	D^{*+}		0.42 ± 0.02	1.17 ± 0.01	93.2/16
pp, 7000	D^0		0.49 ± 0.02	1.15 ± 0.01	7.5/10
	D^+		0.47 ± 0.04	1.16 ± 0.01	7.8/8
	D^{*+}		0.44 ± 0.04	1.17 ± 0.01	7.5/8

Nevertheless, there are differences between the values of the Tsallis parameters corresponding to heavy- and light-flavour hadrons. This can give us an insight into the different production mechanisms and timescales. On one hand, D mesons show a stronger dependence on the collision systems and centre-of-mass energies. D mesons from $\sqrt{s_{\text{NN}}} = 200$ GeV Au–Au collisions are located towards the bottom left of the $T - (q - 1)$ diagram, while the points of $\sqrt{s} = 5.02$ TeV and 7 TeV collisions can be found towards the top right part of the diagram. This may be explained by the fact that in small systems, c quarks come directly from the early stages of the collisions, corresponding to high T values as well as larger non-extensivity parameter q . On the other hand, in A–A collisions c quarks may experience coalescence within the cooling and expanding medium [43], therefore showing smaller Tsallis parameter values.

Another feature of the Tsallis-thermometer of light-flavour hadrons was the grouping of

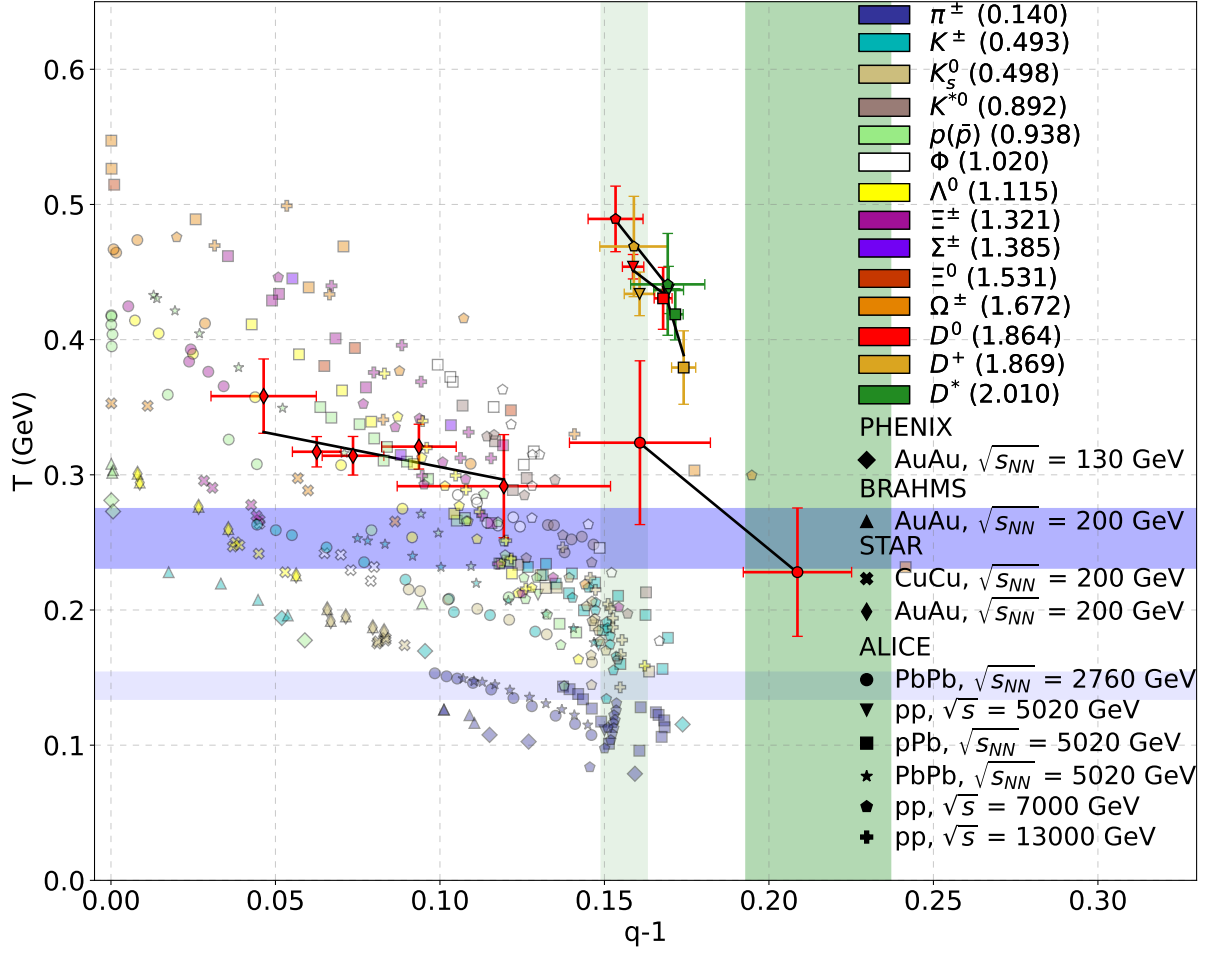


FIG. 2. Tsallis-thermometer: the fitted T and q parameters of identified D^0 , D^+ and D^{*+} mesons stemming from pp, p-Pb, Pb-Pb, and Au-Au collisions at various energies and various multiplicity classes. Results for light-flavour hadrons from [23] are shown in semi-transparent colours for comparison.

all the hadrons at small multiplicities around specific common T_{eq} and q_{eq} values. For the D mesons, the behaviour is similar, however, both the common Tsallis parameter values are higher. To determine these, we used the correlation, Eq. (4) to fit different sets of D meson data. Since D meson species have similar masses (1.864 GeV for D^0 , 1.869 GeV for D^+ and 2.010 GeV for D^{*+}), and data are limited, we considered them as one 'general type' D meson here. Each of the collision systems and energies (pp 5.02 TeV, pp 7 TeV and p-Pb 5.02 TeV) were used in this sense, by providing enough high accuracy for our conclusions.

The fitted correlation between the parameters E and δ^2 are presented in the E — $E\delta^2$

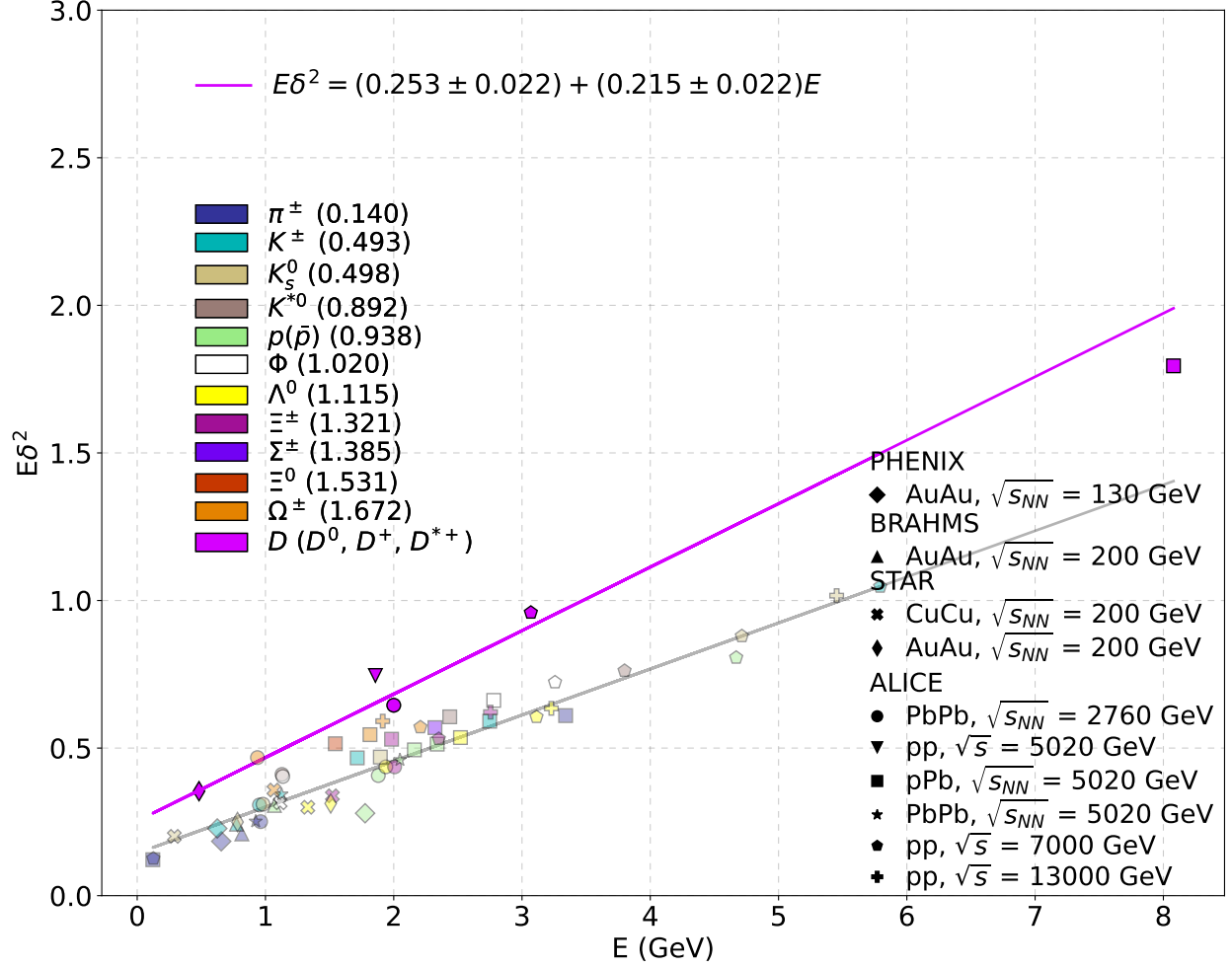


FIG. 3. Correlation of the fit parameters $E\delta^2$ as a function of E . D-meson results (magenta) are compared to light-flavour hadron results (semi-transparent) from [23].

diagram in Fig. 3. The points from fits to the D mesons are compared to those from fits to the light-flavour hadrons, with the uncertainties omitted from the figure for better visibility. One can observe that the relative size of the multiplicity fluctuations δ^2 is larger for all D meson points compared to the light-flavour hadrons. Furthermore, the points from all fits to small systems correspond to larger E values than those from heavy-ion collisions, as the fit determined by these points in the $T-(q-1)$ diagram is steeper.

To find the values of the common Tsallis parameters for D mesons, we inverted the Eq. (4) to the form of

$$E\delta^2 = T - (q-1)E. \quad (6)$$

After fitting D-meson points with this equation we got the values $T_{\text{eq}} = 0.253 \pm 0.022$ GeV

and $q_{\text{eq}} = 1.215 \pm 0.022$. These values together with their uncertainties are shown in Fig. 2 as the blue and the green band, respectively. Therefore, values of the common Tsallis parameters for D mesons are offset by $\Delta T_{\text{eq}} = 0.109 \pm 0.024$ GeV and $\Delta q_{\text{eq}} = 0.059 \pm 0.023$ compared to the light hadrons. This difference, illustrated in Fig. 1 as ΔT , can be explained by the different information which is carried by light and heavy-flavour hadrons. Light flavour is predominantly formed during the kinetic freeze-out phase of a collision, while D mesons are formed by the c quarks, which originate in the early stages of the collisions. Therefore D mesons are probes of a much hotter medium, such as the QGP, which results in an increased Tsallis-temperature value.

The Tsallis temperature T_{eq} obtained separately for light-flavour hadrons and D mesons from the non-extensive thermodynamical model provide an opportunity to connect the initial proper time corresponding to charm creation, τ_{D} to that of light flavour, τ_{LF} . In order to estimate the difference in the production time, a simple Bjorken model can be assumed as the expansion mechanism of the ideal, ultra-relativistic matter, in which the proper-time evolution of the energy density, $\varepsilon = 3P = \sigma T^4$ is given [44, 45], and with the $\varepsilon(\tau_0) = \varepsilon_0 \rightarrow T(\tau_0) = T_0$ initial condition, this has an analytic solution [46]:

$$\tau = \tau_0 \left(\frac{T_0}{T} \right)^3. \quad (7)$$

Assuming the same initial conditions for the light- and heavy-flavour hadrons, $T_{0,\text{LF}}(\tau_0) = T_{0,\text{D}}(\tau_0)$, the following ratio can be obtained:

$$\tau_{\text{D}} = \tau_{\text{LF}} \left(\frac{T_{\text{LF}}}{T_{\text{D}}} \right)^3. \quad (8)$$

Substituting the appropriate T_{eq} values we get $\tau_{\text{D}} = (0.18 \pm 0.06)\tau_{\text{LF}}$, which shows that heavy-flavour hadrons bring thermodynamical information from significantly earlier times of the reaction than light-flavour hadrons as demonstrated in Fig. 4.

The Bjorken expansion can be calculated using a Tsallis-distribution utilizing a time-dependent q parameter [17]. Our result of $q_{\text{eq,D}} > q_{\text{eq,LF}}$ supports their conclusions on the decreasing value of the non-extensivity parameter with increasing τ . In the current model, the change of the value, $\Delta q = 0.059 \pm 0.023$, represents a softening of the transverse momentum distribution between charm and light flavour, therefore it is a sensitive parameter of the time evolution as well.

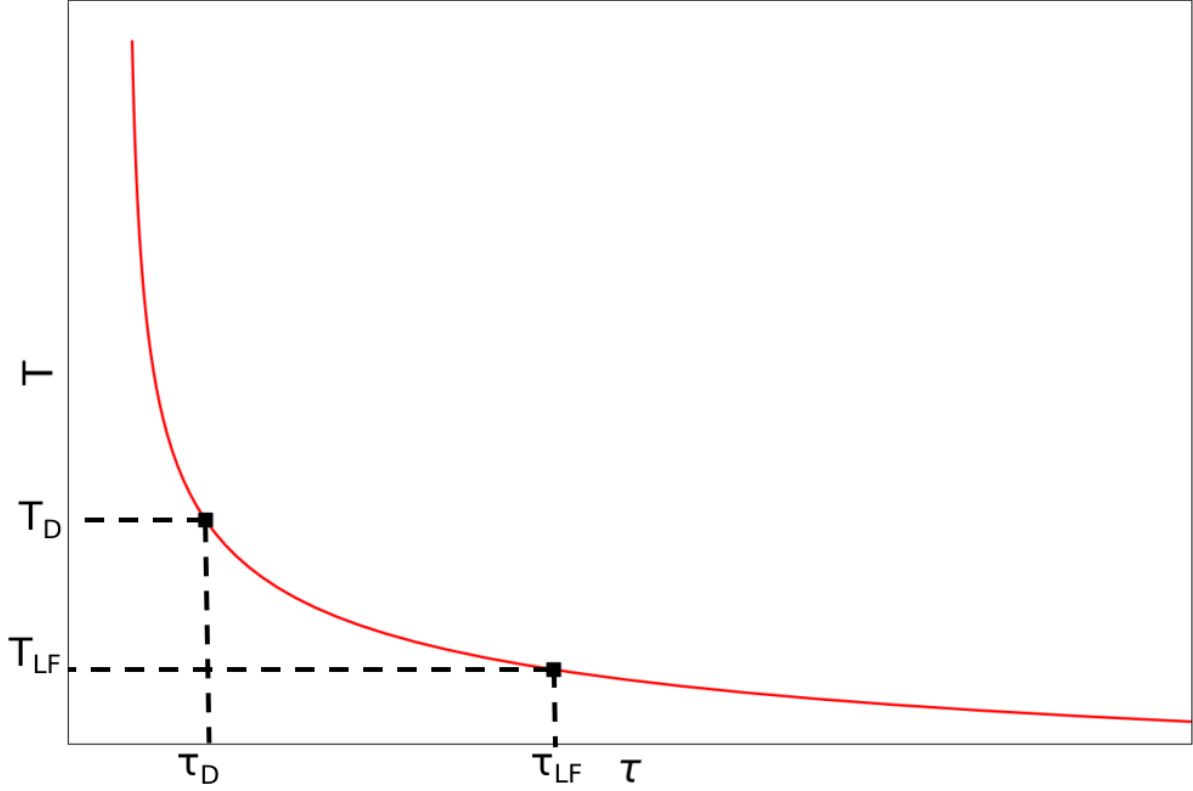


FIG. 4. Schematic cooling curve of an ultrarelativistic collision of hadrons. Temperature and time scales are shown in arbitrary units.

SUMMARY

In this paper we applied the Tsallis–Pareto non-extensive statistical framework to study the properties of D mesons. We showed that the transverse momentum distributions of heavy-flavoured D mesons are well described by the Tsallis–Pareto distribution, thus showing that it can be applied beyond the light flavours. The parameters from the fits fulfil thermodynamical consistency, therefore the statistical framework is applicable to D mesons as well. Similarly to the light-flavour case, the Tsallis parameters of the fits to D-meson data exhibit a scaling behaviour with charged particle multiplicity and with the collision energy. However, we showed that the scaling of D mesons is quantitatively different from that of light-flavour and strange hadrons.

According to our hypothesis, T_{eq} and q_{eq} parameters were found to be higher for heavy-flavour than light-flavour hadrons. The higher q_{eq} means that the correlation within the heavy-quark system is slightly larger than that of light and strange quarks. This is due to

the heavy quarks being produced in the early stages of a collision, where the volume of the system is smaller, while the energy density is higher. The T_{eq} parameter for D mesons is also higher. This can be explained with the similar reasoning, as coming from a much hotter state of the system, D mesons preserve this information, unlike the light-flavour hadrons.

Assuming an expanding system and considering the results from the non-extensive statistical framework, ΔT and Δq on the Tsallis thermometer can be understood as time-frame projections of the different stages of the time evolution. Comparing charm production to that of light flavour, we get that the production of D mesons corresponds to a significantly earlier proper time than light-flavour hadrons, $\tau_D = (0.18 \pm 0.06)\tau_{\text{LF}}$.

Appendix A: Fits on D spectra

Fig. 5 shows the Tsallis fits for D-meson spectra from Refs. [37–41].

Appendix B: Thermodynamical consistency

The quantities in Eq. (5) are calculated from Eq. (1) as the followings, using the fitted Tsallis parameters:

$$P = g \int \frac{d^3p}{(2\pi)^3} T f, \quad (\text{B1})$$

$$N = nV = gV \int \frac{d^3p}{(2\pi)^3} f^q, \quad (\text{B2})$$

$$s = g \int \frac{d^3p}{(2\pi)^3} \left[\frac{m_T - m}{T} f^q + f \right], \quad (\text{B3})$$

$$\varepsilon = g \int \frac{d^3p}{(2\pi)^3} m_T f, \quad (\text{B4})$$

Figure 6 shows that the consistency is fulfilled for light-flavour mesons within 1% precision. For heavier hadrons this can deviate slightly more, however, for D mesons it always stays below 8%.

ACKNOWLEDGMENTS

This work has been supported by the NKFIH grants OTKA FK131979 and K135515, as well as by the 2021-4.1.2-NEMZ_KI-2023 projects. The author acknowledges the research

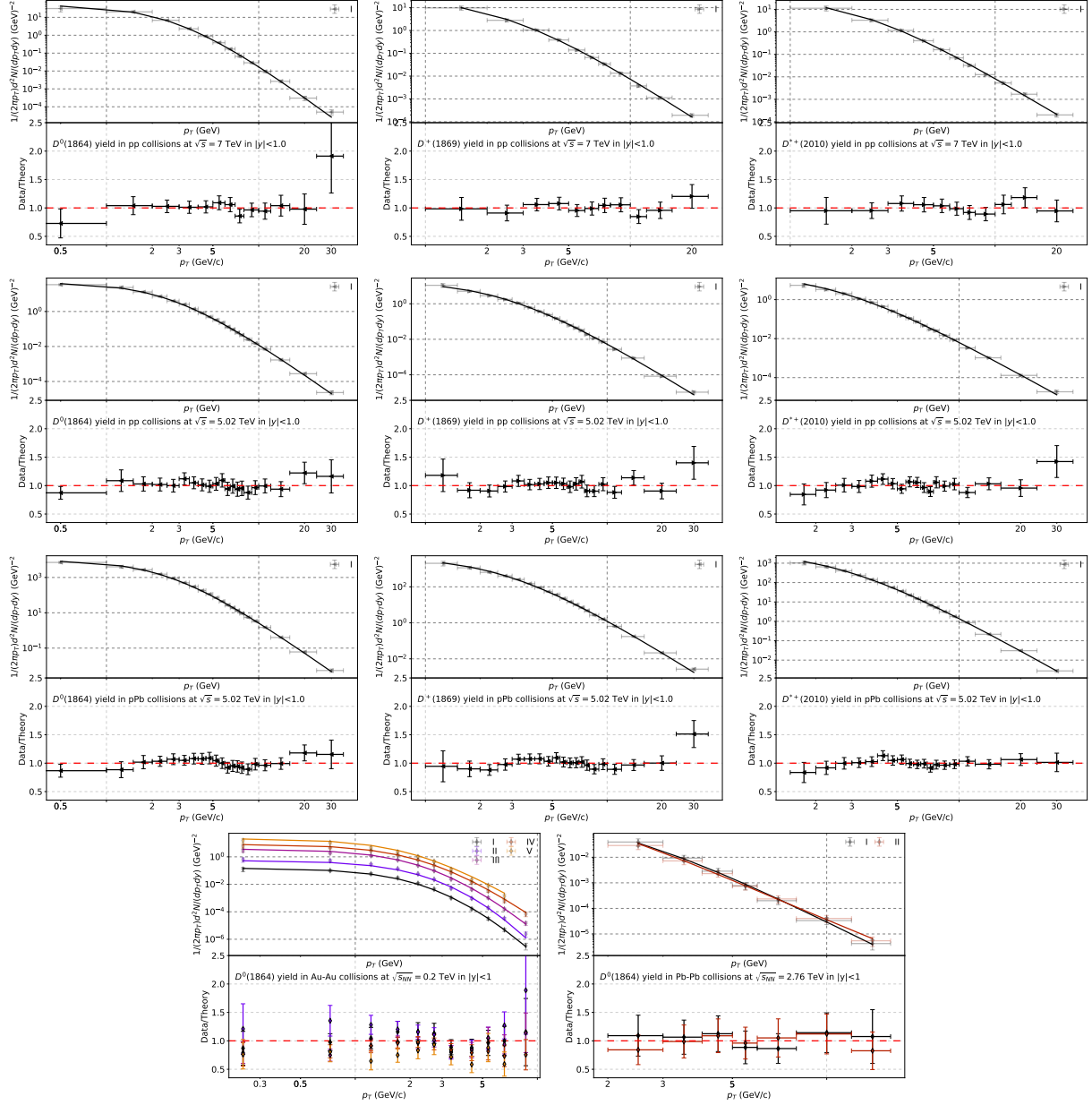


FIG. 5. Fits on the D meson spectra. The upper three rows from top to bottom correspond to ALICE pp data at $\sqrt{s} = 7$ TeV [37], pp collisions at $\sqrt{s} = 5.02$ TeV [38], p-Pb data at $\sqrt{s_{NN}} = 5.02$ TeV [39]. The lowest row shows STAR Au-Au data at $\sqrt{s_{NN}} = 200$ GeV (left) [40] and ALICE Pb-Pb data at $\sqrt{s_{NN}} = 2.76$ TeV (right) [41].

infrastructure provided by the Hungarian Research Network (HUN-REN) and the Wigner

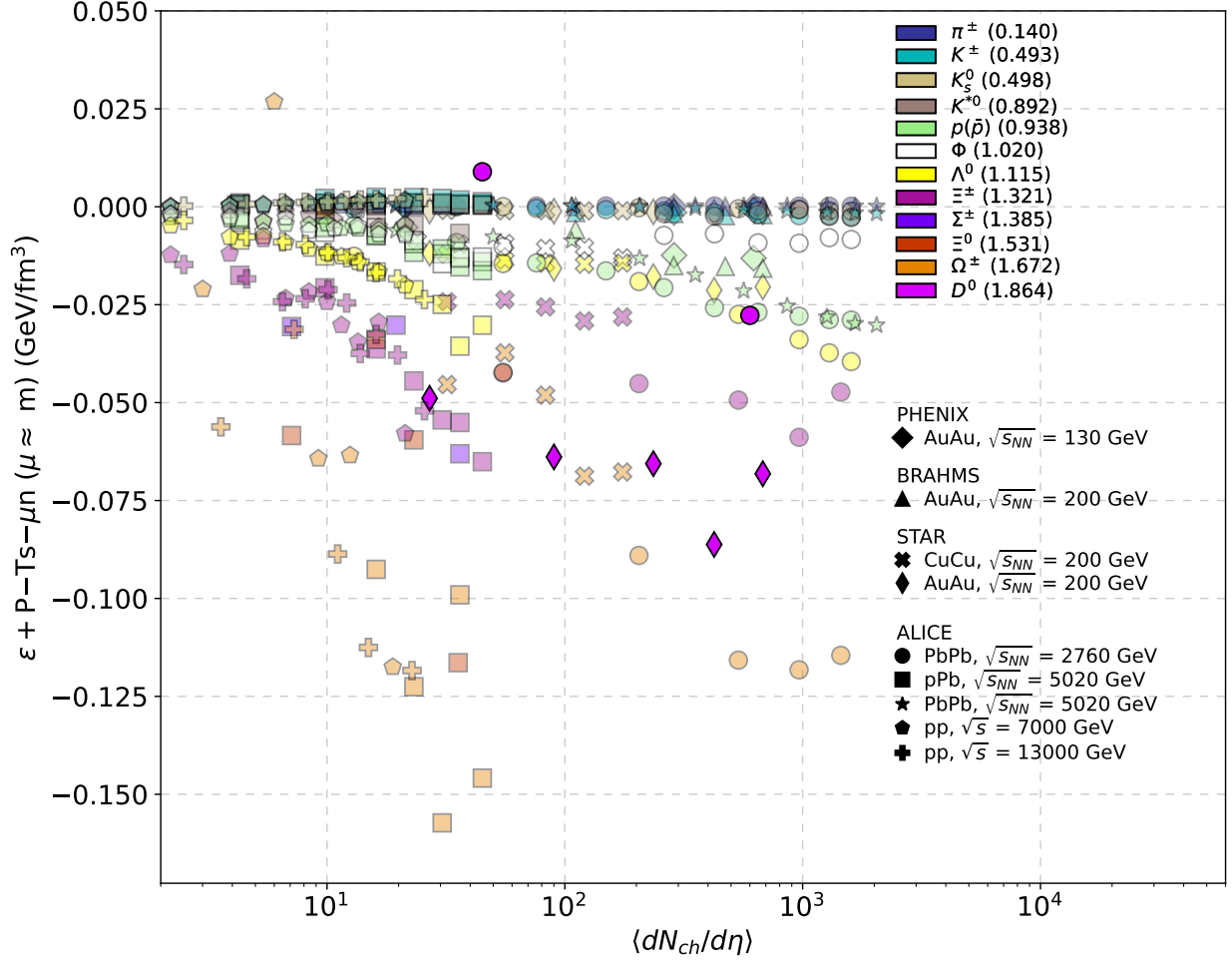


FIG. 6. Thermodynamical consistency of the Tsallis–Pareto parameters. D-meson results (magenta) are compared to light-flavour hadron results from [23] (semi-transparent).

Scientific Computing Laboratory.

-
- [1] LHC Machine, [JINST 3, S08001](#).
 - [2] K. Adcox *et al.* (PHENIX), Formation of dense partonic matter in relativistic nucleus-nucleus collisions at RHIC: Experimental evaluation by the PHENIX collaboration, [Nucl. Phys. A **757**, 184 \(2005\)](#), [arXiv:nucl-ex/0410003](#).
 - [3] J. Adams *et al.* (STAR), Experimental and theoretical challenges in the search for the quark gluon plasma: The STAR Collaboration’s critical assessment of the evidence from RHIC collisions, [Nucl. Phys. A **757**, 102 \(2005\)](#), [arXiv:nucl-ex/0501009](#).

- [4] The ALICE experiment – A journey through QCD, (2022), [arXiv:2211.04384 \[nucl-ex\]](#).
- [5] W. Busza, K. Rajagopal, and W. van der Schee, Heavy Ion Collisions: The Big Picture, and the Big Questions, *Ann. Rev. Nucl. Part. Sci.* **68**, 339 (2018), [arXiv:1802.04801 \[hep-ph\]](#).
- [6] Y. L. Dokshitzer and D. E. Kharzeev, Heavy quark colorimetry of QCD matter, *Phys. Lett. B* **519**, 199 (2001), [arXiv:hep-ph/0106202](#).
- [7] V. Khachatryan *et al.* (CMS), Observation of Long-Range Near-Side Angular Correlations in Proton-Proton Collisions at the LHC, *JHEP* **09**, 091, [arXiv:1009.4122 \[hep-ex\]](#).
- [8] G. Aad *et al.* (ATLAS), Observation of Associated Near-Side and Away-Side Long-Range Correlations in $\sqrt{s_{NN}}=5.02$ TeV Proton-Lead Collisions with the ATLAS Detector, *Phys. Rev. Lett.* **110**, 182302 (2013), [arXiv:1212.5198 \[hep-ex\]](#).
- [9] B. Abelev *et al.* (ALICE), Long-range angular correlations on the near and away side in p -Pb collisions at $\sqrt{s_{NN}} = 5.02$ TeV, *Phys. Lett. B* **719**, 29 (2013), [arXiv:1212.2001 \[nucl-ex\]](#).
- [10] J. Adam *et al.* (ALICE), Enhanced production of multi-strange hadrons in high-multiplicity proton-proton collisions, *Nature Phys.* **13**, 535 (2017), [arXiv:1606.07424 \[nucl-ex\]](#).
- [11] C. Aidala *et al.* (PHENIX), Creation of quark–gluon plasma droplets with three distinct geometries, *Nature Phys.* **15**, 214 (2019), [arXiv:1805.02973 \[nucl-ex\]](#).
- [12] A. Ortiz, G. Bencedi, and H. Bello, Revealing the source of the radial flow patterns in proton–proton collisions using hard probes, *J. Phys. G* **44**, 065001 (2017), [arXiv:1608.04784 \[hep-ph\]](#).
- [13] J. L. Nagle and W. A. Zajc, Small System Collectivity in Relativistic Hadronic and Nuclear Collisions, *Ann. Rev. Nucl. Part. Sci.* **68**, 211 (2018), [arXiv:1801.03477 \[nucl-ex\]](#).
- [14] A. Andronic, P. Braun-Munzinger, K. Redlich, and J. Stachel, Decoding the phase structure of QCD via particle production at high energy, *Nature* **561**, 321 (2018), [arXiv:1710.09425 \[nucl-th\]](#).
- [15] A. Andronic *et al.*, Heavy-flavour and quarkonium production in the LHC era: from proton–proton to heavy-ion collisions, *Eur. Phys. J. C* **76**, 107 (2016), [arXiv:1506.03981 \[nucl-ex\]](#).
- [16] B. Sahoo, S. Deb, and R. Sahoo, Multiplicity, transverse momentum and pseudorapidity dependence of open-heavy flavored hadron production in proton+proton collisions at $\sqrt{s}=13$ TeV, (2022), [arXiv:2208.10901 \[hep-ph\]](#).
- [17] M. Alqahtani, N. Demir, and M. Strickland, Nonextensive hydrodynamics of boost-invariant plasmas, *Eur. Phys. J. C* **82**, 973 (2022), [arXiv:2203.14968 \[nucl-th\]](#).

- [18] Letter of Intent for an ALICE ITS Upgrade in LS3, (2019).
- [19] Letter of intent for ALICE 3: A next-generation heavy-ion experiment at the LHC, (2022), [arXiv:2211.02491 \[physics.ins-det\]](#).
- [20] C. Tsallis, Possible Generalization of Boltzmann-Gibbs Statistics, *J. Statist. Phys.* **52**, 479 (1988).
- [21] C. Tsallis, Nonadditive entropy: The Concept and its use, *Eur. Phys. J. A* **40**, 257 (2009), [arXiv:0812.4370 \[physics.data-an\]](#).
- [22] C. Tsallis, *Introduction to Nonextensive Statistical Mechanics: Approaching a Complex World* (Springer, New York, 2009).
- [23] G. Bíró, G. G. Barnaföldi, and T. S. Bíró, Tsallis-thermometer: a QGP indicator for large and small collisional systems, *J. Phys. G* **47**, 105002 (2020), [arXiv:2003.03278 \[hep-ph\]](#).
- [24] J. Cleymans and H. Satz, Thermal hadron production in high-energy heavy ion collisions, *Z. Phys. C* **57**, 135 (1993), [arXiv:hep-ph/9207204](#).
- [25] P. Braun-Munzinger, K. Redlich, and J. Stachel, Particle production in heavy ion collisions, *Phys. Lett. B* **542**, 491 (2003), [arXiv:nucl-th/0304013](#).
- [26] C.-Y. Wong, G. Wilk, L. J. L. Cirto, and C. Tsallis, From QCD-based hard-scattering to nonextensive statistical mechanical descriptions of transverse momentum spectra in high-energy pp and $p\bar{p}$ collisions, *Phys. Rev. D* **91**, 114027 (2015), [arXiv:1505.02022 \[hep-ph\]](#).
- [27] J. Cleymans, G. I. Lykasov, A. S. Parvan, A. S. Sorin, O. V. Teryaev, and D. Worku, Systematic properties of the Tsallis Distribution: Energy Dependence of Parameters in High-Energy p-p Collisions, *Phys. Lett. B* **723**, 351 (2013), [arXiv:1302.1970 \[hep-ph\]](#).
- [28] K. Shen, G. G. Barnaföldi, and T. S. Bíró, Hadron Spectra Parameters within the Non-Extensive Approach, *Universe* **5**, 122 (2019), [arXiv:1905.08402 \[hep-ph\]](#).
- [29] J. Cleymans and M. Wellington Paradza, Tsallis Statistics in High Energy Physics: Chemical and Thermal Freeze-Outs, *MDPI Physics* **2**, 654 (2020), [arXiv:2101.09490 \[hep-ph\]](#).
- [30] P.-P. Yang, M.-Y. Duan, F.-H. Liu, and R. Sahoo, Analysis of Identified Particle Transverse Momentum Spectra Produced in pp, p-Pb and Pb-Pb Collisions at the LHC Using TP-like Function, *Symmetry* **14**, 1530 (2022), [arXiv:2112.13223 \[hep-ph\]](#).
- [31] J. Gu, C. Li, Q. Wang, W. Zhang, and H. Zheng, Collective expansion in pp collisions using the Tsallis statistics, *J. Phys. G* **49**, 115101 (2022), [arXiv:2201.02091 \[nucl-th\]](#).

- [32] J.-Y. Chen, M.-Y. Duan, F.-H. Liu, and K. K. Olimov, Multi-source thermal model describing multi-region structure of transverse momentum spectra of identified particles and parameter dynamics of system evolution in relativistic collisions [10.1007/s12648-023-03003-4](https://doi.org/10.1007/s12648-023-03003-4) (2023), [arXiv:2310.10227 \[hep-ph\]](https://arxiv.org/abs/2310.10227).
- [33] M. Badshah, A. Haj Ismail, M. Waqas, M. Ajaz, M. U. Mian, E. A. Dawi, M. Adil Khan, and A. AbdelKader, Excitation Function of Freeze-Out Parameters in Symmetric Nucleus–Nucleus and Proton–Proton Collisions at the Same Collision Energy, *Symmetry* **15**, 1554 (2023).
- [34] T. S. Biró, P. Ván, G. G. Barnaföldi, and K. Ürmössy, Statistical power law due to reservoir fluctuations and the universal thermostat independence principle, *Entropy* **16**, 6497 (2014).
- [35] T. S. Biro, G. G. Barnaföldi, and P. Van, New Entropy Formula with Fluctuating Reservoir, *Physica A* **417**, 215 (2015), [arXiv:1405.3813 \[cond-mat.stat-mech\]](https://arxiv.org/abs/1405.3813).
- [36] G. Biró, G. G. Barnaföldi, T. S. Biró, K. Ürmössy, and A. Takács, Systematic Analysis of the Non-extensive Statistical Approach in High Energy Particle Collisions - Experiment vs. Theory, *Entropy* **19**, 88 (2017), [arXiv:1702.02842 \[hep-ph\]](https://arxiv.org/abs/1702.02842).
- [37] S. Acharya *et al.* (ALICE), Measurement of D-meson production at mid-rapidity in pp collisions at $\sqrt{s} = 7$ TeV, *Eur. Phys. J. C* **77**, 550 (2017), [arXiv:1702.00766 \[hep-ex\]](https://arxiv.org/abs/1702.00766).
- [38] S. Acharya *et al.* (ALICE), Measurement of D^0 , D^+ , D^{*+} and D_s^+ production in pp collisions at $\sqrt{s} = 5.02$ TeV with ALICE, *Eur. Phys. J. C* **79**, 388 (2019), [arXiv:1901.07979 \[nucl-ex\]](https://arxiv.org/abs/1901.07979).
- [39] S. Acharya *et al.* (ALICE), Measurement of prompt D^0 , D^+ , D^{*+} , and D_s^+ production in p–Pb collisions at $\sqrt{s_{NN}} = 5.02$ TeV, *JHEP* **12**, 092, [arXiv:1906.03425 \[nucl-ex\]](https://arxiv.org/abs/1906.03425).
- [40] J. Adam *et al.* (STAR), Centrality and transverse momentum dependence of D^0 -meson production at mid-rapidity in Au+Au collisions at $\sqrt{s_{NN}} = 200$ GeV, *Phys. Rev. C* **99**, 034908 (2019), [arXiv:1812.10224 \[nucl-ex\]](https://arxiv.org/abs/1812.10224).
- [41] B. Abelev *et al.* (ALICE), Suppression of high transverse momentum D mesons in central Pb-Pb collisions at $\sqrt{s_{NN}} = 2.76$ TeV, *JHEP* **09**, 112, [arXiv:1203.2160 \[nucl-ex\]](https://arxiv.org/abs/1203.2160).
- [42] M. N. et al., ‘lmfit/lmfit-py 1.0.0’, Zenodo [10.5281/zenodo.3588521](https://doi.org/10.5281/zenodo.3588521) (2019).
- [43] S. Plumari, V. Minissale, S. K. Das, G. Coci, and V. Greco, Charmed Hadrons from Coalescence plus Fragmentation in relativistic nucleus-nucleus collisions at RHIC and LHC, *Eur. Phys. J. C* **78**, 348 (2018), [arXiv:1712.00730 \[hep-ph\]](https://arxiv.org/abs/1712.00730).
- [44] J. D. Bjorken, Highly Relativistic Nucleus-Nucleus Collisions: The Central Rapidity Region, *Phys. Rev. D* **27**, 140 (1983).

- [45] R. Vogt, Chapter 5 - hydrodynamics, in *Ultrarelativistic Heavy-Ion Collisions*, edited by R. Vogt (Elsevier Science B.V., Amsterdam, 2007) pp. 221–278.
- [46] V. K. Magas, J. Gordillo, D. Strottman, Y. L. Xie, and L. P. Csernai, Initial state with shear in peripheral heavy ion collisions, *Phys. Rev. C* **97**, 064903 (2018), [arXiv:1712.00283 \[nucl-th\]](#).